

**Military Technical College**  
**Kobry El-Kobbah,**  
**Cairo, Egypt.**



**18<sup>th</sup> International Conference**  
**on Applied Mechanics and**  
**Mechanical Engineering.**

## **DESIGN OF AN AUTONOMOUS ROBOT OPERATING IN DIFFERENT ENVIRONMENTS**

M. M. H. Alsherif<sup>1</sup>, A. F. Barakat<sup>2</sup> and R. M. Darwish<sup>3</sup>

### **ABSTRACT**

Current autonomous robots are limited to work only in one single environment. For example (swimming and submerging) in water, (walking, jumping and mobile) on ground or (flying and floating) in air. However, in case of seeking a series of autonomous operations that required to be held in different environments, either many robots should be used, or a single robot that can operate in different environments should be established. Therefore, this research is aimed at designing a single autonomous robot that can fly in air -as Unmanned Arial Vehicle (UAV)-, sail in water -as Unmanned Surface Vehicle (USV)- and move on the ground-as Unmanned Ground Vehicle (UGV)- and this is a new category of robots which could be called Unmanned Multi-environments Vehicle or Autonomous Multi-environments Robot. The mathematical model of the proposed robot is derived using kinematic and dynamic model. Then a linearized version of the model is obtained. The used control approach is based on the linear proportional derivative Integral controller (PID) using nested control loops and applied to the model. Finally the behavior of the Robot under the proposed control strategy is simulated and observed in 3D plot Simulink / Matlab.

### **KEY WORDS**

UAV, UGV, USV, 6DOF, 3DOF, PID, Autonomous system

- 
- 1 M. Sc. researcher, Dept. of Mechatronics Engineering, Faculty of Engineering Helwan University, Cairo, Egypt
  - 2 Prof. Dr., Dept. of Mechanical Engineering, Faculty of Engineering, Helwan University, Cairo, Egypt.
  - 3 Lecturer, Dept. of Mechanical Engineering, Faculty of Engineering, Helwan University, Cairo, Egypt.

## NOMENCLATURE

|                                 |   |
|---------------------------------|---|
| $B_y$                           | Distance between the pump and COG of the robot on y-axes  |
| $b$                             | Lift constant factor which measured in ( $N.s^2$ )  |
| $C_A$                           | Coriolis matrix included added mass   |
| $C_{RB}$                        | Matrix of rigid-body Coriolis and centripetal   |
| $D$                             | Damping matrix  |
| $D_l, D_n$                      | Linear and Non-linear damping matrix  |
| $d$                             | Drag constant factor which is measured in ( $N.m.s^2$ )   |
| $F^B = [F_x^B, F_y^B, F_z^B]^T$ | Force affecting the robot in body frame measured in (N)   |
| $F_{gravity}^B$                 | Weight force generated from gravity in body frame   |
| $F_{Thrust}^B$                  | Thrust force generated from actuators in body frame   |
| $F_{air}^B$                     | Air resistance force in body frame  |
| $F_{w\_act}$                    | Force generated from the sailing actuators measured in (N)  |
| $F_{act_x}^B$                   | Sailing actuators forces acting in x direction  |
| $F_{act_y}^B$                   | Sailing actuators forces acting in y direction  |
| $F_{port}$                      | Force generated from port pumps.  |
| $F_{stbd}$                      | Force generated from starboard pumps.   |
| $F_{wind}^B$                    | Wind forces acting on robot   |
| $F_{waves}^B$                   | Waves forces acting on robot  |
| $g$                             | Gravity acceleration ( $= 9.8 m/s^2$ ).   |
| $I$                             | Inertia tensor which measured in ( $N.m.s^2$ )  |
| $J$                             | Angular transformation matrix from body angular velocity to Euler angles rates  |
| $L$                             | Axial distance between right and left rear wheels   |
| $l$                             | Distance between the rotor and COG of the robot   |
| $M^B = [M_x^B, M_y^B, M_z^B]^T$ | Moment affecting the robot in body frame which measured in (N.m)  |
| $M_{gC}^B$                      | Propeller gyro effect moment in x, y axis represented in $M_{pgx}, M_{pgy}$ and inertial counter torque represented in “ $M_{ICz}$ ”. |
| $M_{actx}$                      | Roll moments generated from actuators   |
| $M_{acty}$                      | Pitch moments generated from actuators  |
| $M_{actz}$                      | Yaw moments generated from actuators  |
| $M_{RB}$                        | The rigid-body inertia matrix   |
| $M_{act_z}^B$                   | Sailing actuators moment acting around z-axis measured in (N.m)   |
| $M_{wind}^B$                    | Wind moment acting on robot measured in (N.m)   |
| $M_{waves}^B$                   | Waves moment acting on robot measured in (N.m)  |
| $M_A$                           | Added mass  |
| $m$                             | Robot’s mass measured in (Kg)   |
| $n_p, n_s$                      | Pump’s RPM on the port side and starboard side  |
| $R_B^E$                         | Rotation matrix from body frame to earth frame  |
| $R$                             | Radius of wheel which measured in (m)   |

|   |   |
|---|---|
| $\tau_{\text{ext}}$                           | Total external acting force and moments   |
| $\tau_{hs}^B = [F_{hs}^B \ M_{hs}^B]^T$       | Hydrostatic forces and moments  |
| $\tau_{hyd}^B = [F_{hyd}^B \ M_{hyd}^B]^T$    | Hydrodynamic forces and moments   |
| $V^E = [\dot{x}^E \ \dot{y}^E \ \dot{z}^E]^T$ | Linear velocity of the in earth frame measured in (m/s)   |
| $V^B = [u \ v \ w]^T$                         | Linear velocity of the in body frame measured in (m/s)  |
| $\omega^B = [p \ q \ r]^T$                    | Angular velocity in body frame measured in (rad/s)  |
| $\omega_l, \ \omega_r$                        | Angular velocities of the rear left and right wheel which measured in (r/s)                                       |
| $\Omega$                                      | Angular velocity of rotor i which measured in (rad/s)   |
| $(euler) = [\phi \ \theta \ \psi]^T$          | Angular velocity in earth frame measured in (rad/s) and $(\phi, \theta, \psi)$ are Euler angles measured in (rad) |

## INTRODUCTION

The future wars, automations and manufacturing will completely depend on robots and the human intervention may be limited. So there have been huge evolutions in robots technology in the last few years. The robots will be an essential part in our daily life, they will exist in every house, factory, company, army, etc. The most popular robots are designed to operate only in one single environment (e.g. air, water or ground). The Arial robots could fly, hover or float in air. The water robots could swim, row and submerge in water or jump on water. The ground robots could walk, mobile, jump or roll on ground. However, certain categories of applications required the manipulating of more than one environment. So in such case, many robots are required each for a specific environment. Then the operated robots must cooperate all together to accomplish their overall task. Herein, the concept of autonomous multi-environment robots that can operate in different environments emerge as a comprehensive solution for that challenge. This new devised trend of robots could be used for surveillence, search and rescue missions, planets exploration missions like NASA mars missions, Inspection of gas and oil pipes in water and on the ground.

Therefore, this research concentrates on design, modeling and controlling of an autonomous robot that can fly in air, sail in water and move on ground. The mathematical model of the robot is derived using kinematic and dynamic model. This research area is facing some challenges especially in control field because the proposed robot is under actuated and complicated multivariable nonlinear system. So these systems should be linearized and could be used metaphorically as linear system. The control system is based on linear PID controller, according to its simple structure and its good performance which is acceptable for the proposed robot behavior's control. A 3D SolidWorks model of the robot is shown in Fig.1.

## PROPOSED DESIGNED ROBOT

The proposed robot configuration is a hybrid between UAV as flying robot, UGV as mobile robot and USV as water robot. The robot has ability to operate in different environments but not in the same time. Every environment's actuators are active when the other actuators are not. The motions of the robot in different environments

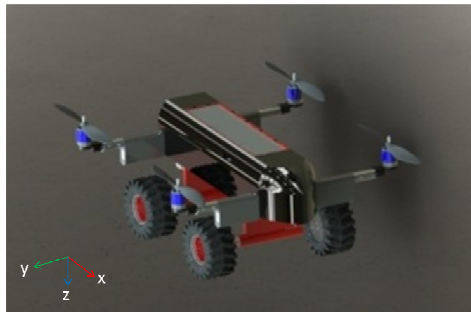


Fig. 1. 3D solidwork model of proposed Multi-environment robot.

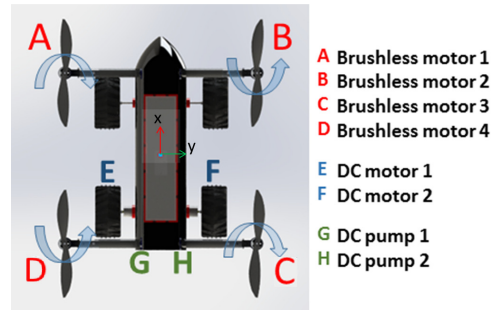


Fig. 2. Motion generators of the robot.

are generated by eight actuators as shown in Fig.2. The robot can fly in air environment as Quadrotor by using four DC brushless motors “A,B,C,D”. It is classified as vertical takeoff and landing aircraft ‘VTOL’. The robot can move on ground by using four wheels with two DC motors “E,F” as differential drive mobile robot.

It also capable to sail in water by using two DC pumps “G,H” as differential drive water robot. The robot motions according to changing in actuators’ speed have been summarized in Table I according to right hand rule. The following design assumptions has been taken: (The Robot is a rigid body and is symmetric around x and y axis’s - In Flying system, the thrust and drag force are proportional to square of propellers’ speed - In mobile system, there is no slipping in x-axis and the wheel is perpendicular to ground - In sailing system, the COG location is the same for COB in x and y axis and the robot surges in calm water).

The main components of the Robot system are summarized in Fig.3 and Electronic diagram structure of the autonomous robot is shown in Fig.4. The LIPO battery is selected as power source which is carried inside the robot.

TABLE 1. THEORY OF MOTION IN DIFFERENT ENVIRONMENTS

| Motions   | Environments |    |    |    |        |    |       |    |
|-----------|--------------|----|----|----|--------|----|-------|----|
|           | Air          |    |    |    | Ground |    | water |    |
| Actuators | A            | B  | C  | D  | E      | F  | G     | H  |
| Forward   | -            | -  | -  | -  | +1     | +1 | +1    | +1 |
| Backward  | -            | -  | -  | -  | -1     | -1 | -     | -  |
| Up        | +2           | +2 | +2 | +2 | -      | -  | -     | -  |
| Down      | +1           | +1 | +1 | +1 | -      | -  | -     | -  |
| Roll +ve  | +2           | +1 | +1 | +2 | -      | -  | -     | -  |
| Roll -ve  | +1           | +2 | +2 | +1 | -      | -  | -     | -  |
| Pitch +ve | +2           | +2 | +1 | +1 | -      | -  | -     | -  |
| Pitch -ve | +1           | +1 | +2 | +2 | -      | -  | -     | -  |
| Yaw +ve   | +1           | +2 | +1 | +2 | +1     | -1 | +1    | 0  |
| Yaw -Ve   | +2           | +1 | +2 | +1 | -1     | +1 | 0     | +1 |

## ROBOT MODELING

The mathematical model of the robot for the indented environments (i.e., air, ground and water) is defined independently. Then, they are merged and enrolled in control process. There are two different coordinate frames are used to represent position and orientation of the robot. Firstly, the “earth frame” is a fixed frame used as reference. Its’ x, y, z axis’s are pointed to North, East and the center of the Earth directions respectively. Secondly, the “body frame” has its origin fixed to the center

### Mechanical Component

- 1 Frame, 4 Wings
- 4 Pulleys , 1 Seal
- 4 Propellers (APC 10x4.7 CW, CCW)
- 4 Wheels

### Electro-Mechanical Component

- 2 DC motor DAGU (250RPM, 12V)
- 4 Brushless Motor EMAX BL2220 (1200 KV, thrust 1400 g, 11.1 Volt)
- 2 DC Pump (12 Volt)

### Power supply

- 2 Battery (LIPO, 11.1 Volt, 35C, 5200mAh)
- Power distribution board (3.3 Volt, 5 Volt, 9 Volt, 12 Volt)
- Digital to digital converter
- Wires (AWG-16)

### Control Unit

- Microcontroller (Atmega 2560, 5 Volt )



### Life Time

- Flying process (Up to 10 minutes)
- Mobile process (Up to 20 minutes)
- Sailing Process (Up to 20 minutes)

### Electronic Component

- Lighting LEDs (5 Volt)
- Camera (9 Volt)
- Sensors (3.3 Volt) (3 axis Accelerometer "ADXL345") (3 axis Gyroscope "L3G4200D") (3 axis Compass "HMC5883L") (GPS "U-BLOX NEO-6M") (Pressure sensor "BMP085") (water detection "spark fun H2O")
- 2 ESC DC motor (Cytron MD10, 12 Volt)
- 4 ESC Brushless Motor (EMAX 30A, 11.1 Volt )
- 2 ESC DC pump (Cytron MD10, 12 Volt)
- Wireless (5 Volt) (RF Module 915MHZ transceiver) (Camera RF 2.4GHZ transceiver)

Fig. 3. Architecture of the robot.

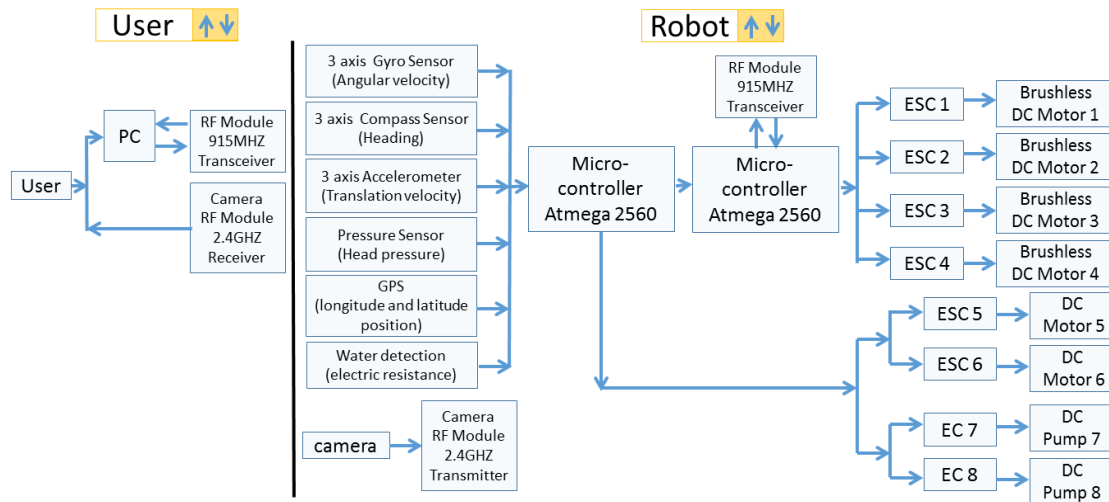


Fig. 4. Electronic diagram structure of the autonomous robot.

of gravity of the robot. Its' x, y, z axis's are pointed to the Robot's forward, right and downward directions respectively.

## Mathematical Model of the Robot

### Kinematic model

The "earth frame" and the "body frame" can be related to each other by rotations relation matrix as shown in the following equations:[1],[9],[12]

$$V^E = R_B^E \cdot V^B \tag{1}$$

$$(\dot{euler}) = J \cdot \omega^B \tag{2}$$

$$R_B^E = \begin{bmatrix} C\theta C\psi & S\phi S\theta C\psi - C\phi S\psi & C\phi S\theta C\psi + S\phi S\psi \\ C\theta S\psi & S\phi S\theta S\psi + C\phi C\psi & C\phi S\theta S\psi - S\phi C\psi \\ -S\theta & S\phi C\theta & C\phi C\theta \end{bmatrix} \tag{3}$$

$$J = \begin{bmatrix} 1 & S\varphi t\theta & C\varphi t\theta \\ 0 & C\varphi & -S\varphi \\ 0 & S\varphi/C\theta & C\varphi/C\theta \end{bmatrix} \quad (4)$$

where S:sin,C:cos,t:tan.

So, the kinematic model of the robot is: (6DOF) [9]

$$\begin{cases} \dot{x}^E = (C\theta C\psi)u + (S\varphi S\theta C\psi - C\varphi S\psi)v + (C\varphi S\theta C\psi + S\varphi S\psi)w \\ \dot{y}^E = (C\theta S\psi)u + (S\varphi S\theta S\psi + C\varphi C\psi)v + (C\varphi S\theta S\psi - S\varphi C\psi)w \\ \dot{z}^E = (-S\theta)u + (S\varphi C\theta)v + (C\varphi C\theta)w \\ \dot{\varphi} = p + (S\varphi t\theta)q + (C\varphi t\theta)r \\ \dot{\theta} = (C\varphi)q + (-S\varphi)r \\ \dot{\psi} = (S\varphi/C\theta)q + (C\varphi/C\theta)r \end{cases} \quad (5)$$

### Dynamic model

Newton-Euler formalism is used to represent the dynamics of a rigid body as expressed in equation. [1], [12]

$$\begin{cases} mI_{3 \times 3} \dot{V}^B + \omega^B \times mV^B = F^B \\ I \dot{\omega}^B + \omega^B \times I \omega^B = M^B \end{cases} \quad (6)$$

$$I = \begin{bmatrix} I_{xx} & 0 & 0 \\ 0 & I_{yy} & 0 \\ 0 & 0 & I_{zz} \end{bmatrix} \quad (7)$$

So, the dynamic model of the robot is: (6DOF)

$$\begin{cases} F_x^B = m\dot{u} + m(qw - rv) \\ F_y^B = m\dot{v} + m(ru - pw) \\ F_z^B = m\dot{w} + m(pv - qu) \\ M_x^B = I_{xx} \dot{p} + (I_{zz} - I_{yy})qr \\ M_y^B = I_{yy} \dot{q} + (I_{xx} - I_{zz})pr \\ M_z^B = I_{zz} \dot{r} + (I_{yy} - I_{xx})pq \end{cases} \quad (8)$$

## Mathematical Model of the Flying System

### Kinematic Model

The kinematic model is as equation 5 [9].

### Dynamic model

The main effecting forces and moments on the flying robot are as follow: [7], [8], [9], [10].

$$F^B = F_{gravity}^B + F_{Thrust}^B + F_{air}^B \quad (9)$$

$$M^B = M_{Actuators}^B + M_{gc}^B \quad (10)$$

$$\begin{bmatrix} F_x^B \\ F_y^B \\ F_z^B \end{bmatrix} = \begin{bmatrix} -mg \sin \theta \\ mg \cos \theta \sin \varphi \\ mg \cos \theta \cos \varphi \end{bmatrix} + \begin{bmatrix} 0 \\ 0 \\ -F_T \end{bmatrix} + \begin{bmatrix} f_{airx}^B \\ f_{airy}^B \\ f_{airz}^B \end{bmatrix} \quad (11)$$

$$\begin{bmatrix} M_x^B \\ M_y^B \\ M_z^B \end{bmatrix} = \begin{bmatrix} M_{actx} \\ M_{acty} \\ M_{actz} \end{bmatrix} + \begin{bmatrix} M_{pgx} \\ M_{pgy} \\ M_{ICz} \end{bmatrix} \quad (12)$$

The forces and moments generated from actuators are [14]:

$$\begin{bmatrix} F_T \\ M_{actx} \\ M_{acty} \\ M_{actz} \end{bmatrix} = \begin{bmatrix} b & b & b & b \\ b.l & -b.l & -bl & bl \\ b.l & b.l & -bl & -bl \\ -d & d & -d & d \end{bmatrix} \begin{bmatrix} \Omega_A^2 \\ \Omega_B^2 \\ \Omega_C^2 \\ \Omega_D^2 \end{bmatrix} \quad (13)$$

By applying equations (11), (12) in equation (8), the dynamic model of the flying system in body frame could be expressed as: (6DOF) [10],[15]

$$\begin{cases} \dot{u} = -g \sin \theta + (f_{airx}^B / m) + (rv - qw) \\ \dot{v} = g \cos \theta \sin \varphi + (f_{airy}^B / m) + (pw - ru) \\ \dot{w} = g \cos \theta \cos \varphi + (f_{airz}^B / m) - (F_T / m) + (qu - pv) \\ \dot{p} = (M_{actx} / I_{xx}) + (M_{pgx} / I_{xx}) - ((I_{zz} - I_{yy}) / I_{xx}) qr \\ \dot{q} = (M_{acty} / I_{yy}) + (M_{pgy} / I_{yy}) - ((I_{xx} - I_{zz}) / I_{yy}) pr \\ \dot{r} = (M_{actz} / I_{zz}) + (M_{ICz} / I_{zz}) - ((I_{yy} - I_{xx}) / I_{zz}) pq \end{cases} \quad (14)$$

### Mathematical Model of the Mobile System

The mobile robot rotates only around z-axis so ( $\varphi = \theta = 0$ ), moving only along x-axis in body frame so ( $v = w = 0$ ) and moving in x-y plane in earth frame so ( $z = 0$ ). So from equation (5) the kinematic model of the mobile system in body frame will be as follows: (3DOF) [2]

$$\begin{cases} \dot{x}^E = (\cos \psi) u \\ \dot{y}^E = (\sin \psi) u \\ \dot{\psi} = r \end{cases} \quad (15)$$

The differential drive robot's linear and angular velocities in body frame can be deduced from angular velocity of the right and left rear wheels of the robot as [24]:

$$u = R \frac{(\omega_l + \omega_r)}{2} \quad (16)$$

$$r = \frac{R}{L}(\omega_l - \omega_r) \quad (17)$$

By applying equations (16) and (17) in equation (15), the final differential derive model would be expressed as: (3DOF)

$$\begin{cases} \dot{x}^E = R \frac{(\omega_l + \omega_r)}{2} \cos \psi \\ \dot{y}^E = R \frac{(\omega_l + \omega_r)}{2} \sin \psi \\ \dot{\psi} = \frac{R}{L}(\omega_l - \omega_r) \end{cases} \quad (18)$$

## Mathematical Model of the Sailing System

### Kinematic model

It is assumed that the sailing robot is rotating only around z-axis so ( $\varphi = \theta = 0$ ), moving only along x-axis and y-axis in body frame so ( $w = 0$ ) and moving in x-y plane in earth frame so ( $z = 0$ ). So from equation (5) the kinematic model of the sailing system in body frame is: (3DOF) [18], [20].

$$\begin{cases} \dot{x}^E = (\cos \psi)u - (\sin \psi)v \\ \dot{y}^E = (\sin \psi)u + (\cos \psi)v \\ \dot{\psi} = r \end{cases} \quad (19)$$

### Dynamic model

The sailing robots' components of motions are shown in Fig 5. It is assumed that the sailing robot maneuvering is generally treated as plane motion with three components surge, sway and yaw. So the dynamic model of the sailing robot can be described in Body frame after simplifying equation (8) as follow: (3DOF) [3],[11],[12],[19],[20],[21].

$$\begin{cases} F_x^B = m(\dot{u} - rv) \\ F_y^B = m(\dot{v} + ru) \\ M_z^B = I_{zz} \dot{r} \end{cases} \quad (20)$$

Also The 3 DOF horizontal plane models for maneuvering are based on the rigid-body kinetics can be described as: [3],[4],[12],[20]

$$\begin{cases} M_{RB} \dot{V} + C_{RB}(V)V = \tau_{ext} \\ V = [u \ v \ r] \end{cases} \quad (21)$$

$$M_{RB} = \begin{bmatrix} m & 0 & 0 \\ 0 & m & mx_g \\ 0 & mx_g & I_z \end{bmatrix} \quad (22)$$

$$C_{RB} = \begin{bmatrix} 0 & 0 & -m(x_g r + v) \\ 0 & 0 & mu \\ m(x_g r + v) & -mu & 0 \end{bmatrix} \quad (23)$$

where  $M_{RB}, C_{RB}, \tau_{ext}$  are the rigid-body inertia matrix, matrix of rigid-body Coriolis and centripetal, the total external acting force and moments.

The main affecting forces and moments on the sailing robot are as follow:  
First, The actuators forces and moments are: [16],[18],[21],[23].

$$\tau_{act}^B = [F_{w_{act}} \ M_{w_{act}}]^T = [F_{act_x}^B \ F_{act_y}^B \ M_{act_z}^B]^T \quad (24)$$

$$\begin{cases} F_{act_x}^B = F_{port} + F_{stbd} \\ F_{act_y}^B = 0 \\ M_{act_z}^B = B_y (F_{port} - F_{stbd}) \end{cases} \quad (25)$$

$$\begin{cases} F_{port} = (F_{act_x}^B / 2) + (M_{act_z}^B / 2 B_y) \\ F_{stbd} = (F_{act_x}^B / 2) - (M_{act_z}^B / 2 B_y) \end{cases} \quad (26)$$

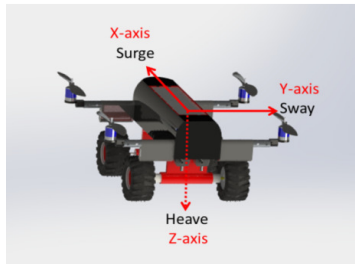


Fig. 5. Sailing robot's components of motions

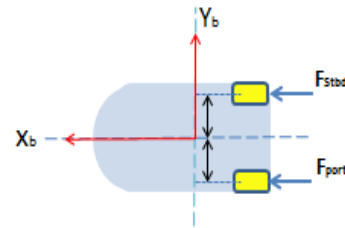


Fig. 6. Rotors and distances to COG.

The robot generates the propulsion forces and turning moment with two thrusters as shown in fig. 6 providing  $n_p$  and  $n_s$  RPM on the port and starboard side respectively. And it is assumed that the thrust has a linear relation with RPM So: [17]

$$\begin{cases} F_{port} = \frac{n_p}{n_{p\_max}} \cdot F_{port\_max} \\ F_{stbd} = \frac{n_s}{n_{s\_max}} \cdot F_{stbd\_max} \end{cases} \quad (27)$$

Second, The hydrostatic forces and moments: In the horizontal plane, the hydrostatic forces and moments  $\tau_{hs}^B$  is assumed to equal zero.

$$\tau_{hs}^B = [F_{hs}^B \ M_{hs}^B]^T = 0 \quad (28)$$

Third, The hydrodynamic forces and moments:

It is supposed that relative velocity is equal normal velocity ( $V_r = V$ ).

The hydrodynamic forces and moments  $\tau_{hyd}^B$  is as follow:

$$\begin{cases} \tau_{hyd}^B = [F_{hyd}^B \quad M_{hyd}^B]^T = -M_A \dot{V} - C_A(V_r)V_r - D(V_r)V_r \\ \tau_{hyd}^B = -M_A \dot{V} - C_A(V)v - D(V)V \end{cases} \quad (29)$$

$$M_A = \begin{bmatrix} -X_{\dot{u}} & 0 & 0 \\ 0 & -Y_{\dot{v}} & -Y_{\dot{r}} \\ 0 & -N_{\dot{v}} & -N_{\dot{r}} \end{bmatrix} \quad (30)$$

$$C_A = \begin{bmatrix} 0 & 0 & Y_{v|v} + Y_{r|r} \\ 0 & 0 & -X_{\dot{u}}u \\ -Y_{v|v} - Y_{r|r} & X_{\dot{u}}u & 0 \end{bmatrix} \quad (31)$$

And [3],[11],[12],[13]

$$D(v) = D_l + D_n = \begin{bmatrix} -X_u & 0 & 0 \\ 0 & -Y_v & -Y_r \\ 0 & -N_v & -N_r \end{bmatrix} + \begin{bmatrix} -X_{u|u}|u| & 0 & 0 \\ 0 & -Y_{v|v}|v| - Y_{v|r}|r| & -Y_{r|v}|v| - Y_{r|r}|r| \\ 0 & -N_{v|v}|v| - N_{v|r}|r| & -N_{r|v}|v| - N_{r|r}|r| \end{bmatrix} \quad (32)$$

where:  $X_{\dot{u}}, Y_{\dot{v}}, N_{\dot{r}}, Y_{\dot{r}}, X_u, Y_v, N_r, Y_r, N_v$  are linear damping coefficients.  $X_{u|u}|u|, Y_{v|v}|v|, Y_{v|r}|r|, Y_{r|v}|v|, Y_{r|r}|r|, N_{v|v}|v|, N_{v|r}|r|, N_{r|v}|v|, N_{r|r}|r|$  are non-linear damping coefficients.

Fourth, Other forces and moments:

$$\begin{cases} \tau_{other}^B = [\tau_{wind}^B \quad \tau_{waves}^B]^T \\ \tau_{other}^B = [F_{wind}^B + F_{waves}^B \quad M_{wind}^B + M_{waves}^B]^T \end{cases} \quad (33)$$

Finally, the total force and moments acting in Robot:

$$\tau^B = \tau_{act}^B + \tau_{hs}^B + \tau_{hyd}^B + \tau_{wind}^B + \tau_{waves}^B \quad (34)$$

where  $\tau_{hs}^B = \tau_{wind}^B = \tau_{waves}^B = 0$  so:

$$\tau^B = \tau_{act}^B + \tau_{hyd}^B = -M_A \dot{V} - C_A(V)V - D(V)V \quad (35)$$

The dynamic model of the robot after offset the acting forces and moments can be described in Body frame simply as follow: (3DOF) [3],[11],[12],[18]

$$(M_{RB} + M_A) \dot{V} + (C_{RB} + C_A)(V)V + D(V)V = \tau_{act}^B \quad (36)$$

## ROBOT CONTROL

PID controller is selected in this research according to the following reasons [5]; (It has a simple structure and is easy to be implemented - It has a good performance and is acceptable for the robot behavior's control - It can be tuned easily).

## Flying System Control

To control the flying Robot many nested control loop structure will be applied. The main controllers are as follow [10],[2]:

1- Altitude Controller: “Fig. 7”: The task of this control is to keep the Robot flying at certain height. It controls the height by increasing and decreasing the net thrust. The derived control law is in equation (39).

2- Attitude Controller: “Fig. 8, 9, 10”. The Attitude controller is contains from three main controllers: (Roll – Pitch – Yaw) controller and their derived laws are in equation (40), (41) and (42) respectively.

3- Position Controller: “Fig. 11, 12”. The x and y position cannot be directly controlled, But it can be controlled by changing roll and pitch angles. To simplify the  $\ddot{x}^E, \ddot{y}^E$  equations at hovering operation where robot weight equals thrust force, It is supposed that: In longitude motion: ( $\varphi = \psi = 0$ ) So ( $\cos \varphi = \cos \psi = 1$ ) and ( $\sin \varphi = \sin \psi = 0$ ). In Latitude motion: ( $\theta = \psi = 0$ ) So ( $\cos \theta = \cos \psi = 1$ ) and ( $\sin \theta = \sin \psi = 0$ ). The simplified equation is shown in equation (37). Also it is supposed that a small angle approximation is used So the final equation is expressed in equation (38). The position derived control laws are equation (43) and (44). [6]

$$\begin{cases} \ddot{x}^E = -\frac{m \cdot g}{m}(\sin \theta) \\ \ddot{y}^E = -\frac{m \cdot g}{m}(-\sin \varphi) \end{cases} \quad (37)$$

$$\begin{cases} \varphi = -\frac{1}{g} \ddot{y}^E \\ \theta = \frac{1}{g} \ddot{x}^E \end{cases} \quad (38)$$

$$\begin{cases} \dot{Z}_{des} = K_{pz} (Z_{des} - Z) \\ F_{Tdes} = K_{pZ} (\dot{Z}_{des} - \dot{Z}) + F_{Tbias} \end{cases} \quad (39)$$

$$\begin{cases} \dot{\varphi}_{des} = K_{p\varphi} (\varphi_{des} - \varphi) \\ M_{actx des} = K_{p\varphi} (\dot{\varphi}_{des} - \dot{\varphi}) \end{cases} \quad (40)$$

$$\begin{cases} \dot{\theta}_{des} = K_{p\theta} (\theta_{des} - \theta) \\ M_{acty des} = K_{p\theta} (\dot{\theta}_{des} - \dot{\theta}) \end{cases} \quad (41)$$

$$\begin{cases} \dot{\psi}_{des} = K_{p\psi} (\psi_{des} - \psi) \\ M_{actz des} = K_{p\psi} (\dot{\psi}_{des} - \dot{\psi}) \end{cases} \quad (42)$$

$$\begin{cases} \dot{X}_{des} = K_{pX} (X_{des} - X) \\ \theta_{des} = K_{p\dot{X}} (\dot{X}_{des} - \dot{X}) \end{cases} \quad (43)$$

$$\begin{cases} \dot{Y}_{des} = K_{pY} (Y_{des} - Y) \\ \Phi_{des} = K_{p\dot{Y}} (\dot{Y}_{des} - \dot{Y}) \end{cases} \quad (44)$$

where:  $Z, X, Y, \varphi, \theta, \psi$  are the measured values.  $Z_{des}, X_{des}, Y_{des}, \varphi_{des}, \theta_{des}, \psi_{des}$  are the desired values.  $\dot{Z}, \dot{X}, \dot{Y}$  are the measured velocity.  $\dot{Z}_{des}, \dot{X}_{des}, \dot{Y}_{des}$  are the desired velocity.  $\dot{\varphi}, \dot{\theta}, \dot{\psi}$  the measured angular rate.  $\dot{\varphi}_{des}, \dot{\theta}_{des}, \dot{\psi}_{des}$  the desired angular rate.  $K_{pz}, K_{p\dot{z}}, K_{p\varphi}, K_{p\dot{\varphi}}, K_{p\theta}, K_{p\dot{\theta}}, K_{p\psi}, K_{p\dot{\psi}}, K_{pX}, K_{p\dot{X}}, K_{pY}, K_{p\dot{Y}}$  are PID gains.  $F_{Tdes}, F_{Tbias}, M_{actx des}, M_{acty des}, M_{actz des}$  are the desired thrust force, bias force, desired roll moment, desired pitch moments and desired yaw moments.

### Mobile System Control

Moving from point to point technique is used to control the mobile Robot. The main controllers are as follow: [24], [2]

1- Throttle Controller “Fig. 13” : The Throttle controller is to control the speed of the robot in longitude motion. The robot’s velocity is controlled using proportional controller applied to the distance from the desired goal point. The derived control laws is in equation (45).

2- Heading Controller “Fig. 14” : The heading controller is the responsible for steering the robot toward the goal point. The derived control law is shown in equation (46).

$$u_{des} = K_{ptXY} \sqrt{(x_{des} - x)^2 + (y_{des} - y)^2} \quad (45)$$

$$\psi_{des} = K_{phXY} \cdot \arctan(y_{des} - y / x_{des} - x) \quad (46)$$

where:  $x, y$  are The measured values.  $X_{des}, Y_{des}, \psi_{des}$  are The desired values.  $K_{ptxy}, K_{phxy}$  are PID gains and  $u_{des}$  is desired velocity.

### Sailing System Control

Moving from point to point technique is also used to control the sailing Robot. The main controllers are as follow: [16],[22]

1- Surge Controller “Fig. 15” : The surge controller is control surge force of the robot in longitude motion. The derived control laws is in equation (47).

2- Heading Controller “Fig. 16” : The heading controller is the responsible for steering the robot toward the goal point by controlling the yaw moment. The derived control laws are in equation (48).

$$\begin{cases} u_{des} = K_{ptXY} \sqrt{(x_{des} - x)^2 + (y_{des} - y)^2} \\ F_{act des} = K_{pa} \cdot u_{des} \end{cases} \quad (47)$$

$$\begin{cases} \psi_{des} = K_{phXY} \cdot \arctan(y_{des} - y / x_{des} - x) \\ \dot{\psi}_{des} = K_{p\psi} (\psi_{des} - \psi) \\ M_{actz des} = K_{p\dot{\psi}} (\dot{\psi}_{des} - \dot{\psi}) \end{cases} \quad (48)$$

where:  $X, Y, \psi$  are The measured values.  $X_{des}, Y_{des}, \psi_{des}$  are The desired values.  $K_{pxy}, K_{phxy}, K_{p\psi}, K_{p\dot{\psi}}$  are PID gains.  $u_{des}$  is desired velocity.  $F_{act\ des}, M_{act\ des}$  are desired surge force and desired yaw moments.

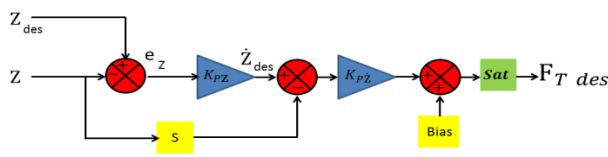


Fig. 7. Flying system: Altitude Controller

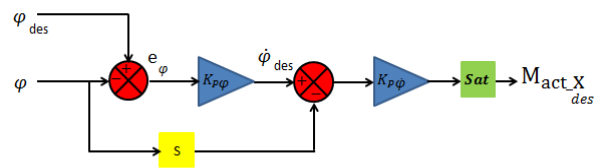


Fig. 8. Flying system: Roll Controller

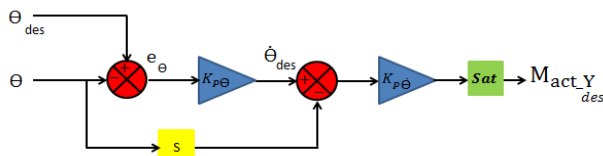


Fig. 9. Flying system: Pitch Controller

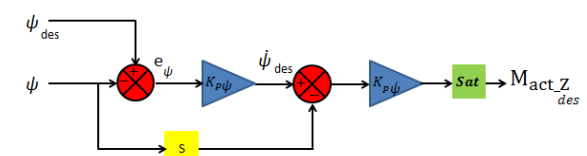


Fig. 10. Flying system: Yaw Controller

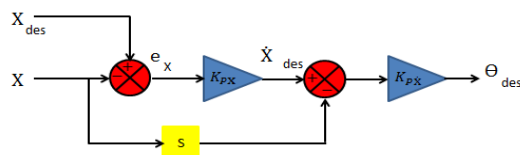


Fig. 11. Flying system: X Controller

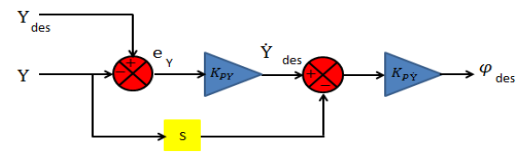


Fig. 12. Flying system: Y Controller

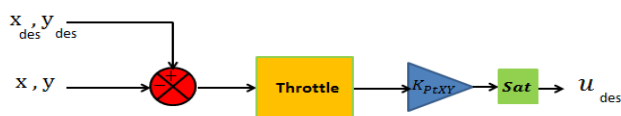


Fig. 13. Mobile system: Position Controller

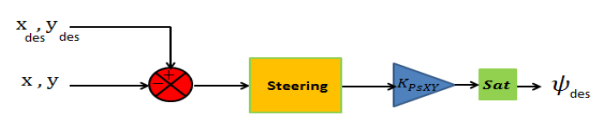


Fig. 14. Mobile system: Heading Controller

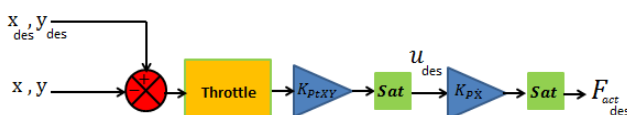


Fig. 15. Sailing system: Position Controller

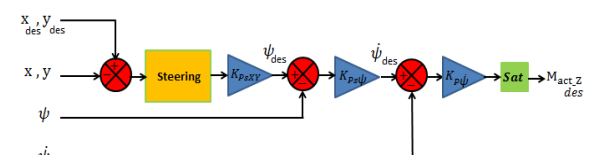


Fig. 16. Sailing system: Heading Controller

## SIMULATION AND RESULTS

The Robot has been simulated in Matlab and the controllers are tested and verified using closed loop simulation. The logic diagram of the robot's total system with corresponding equations is shown in Fig. 17 and the Simulink block of the system is shown in Fig. 18. The Robot simulation parameters are declared in Table 2.

The selected control gains are shown in table 3 and the controllers are under saturations conditions are shown in Table 4. The control response specification's data for full system test with respect to time response is shown in Table 5.

The simulation response of the controllers in: Flying system (are shown in the following: Fig.19 "show the trajectory response of moving the flying robot from point

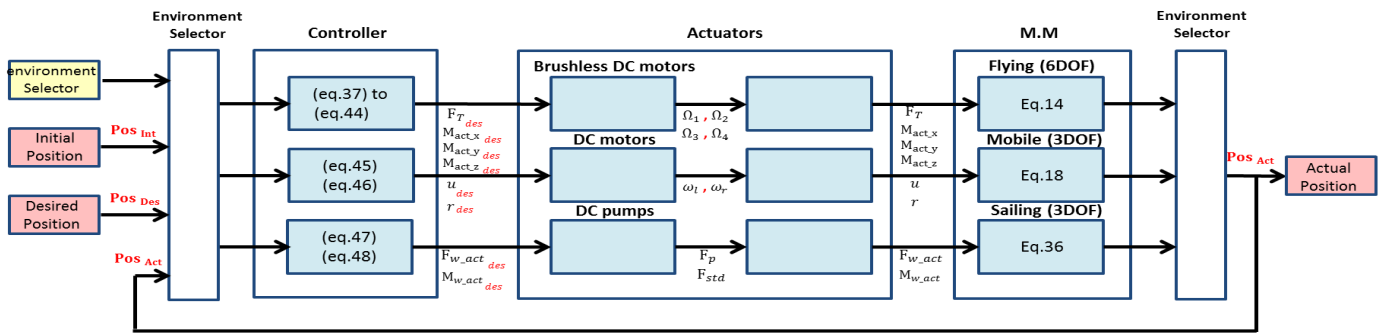


Fig. 17. TOTAL SYSTEM BLOCK DIAGRAM

TABLE 2. ROBOT SIMULATION PARAMETERS

| Parameters | Value | Unit    | Parameters     | Value    | Unit      | Parameters | Value | Unit     |
|------------|-------|---------|----------------|----------|-----------|------------|-------|----------|
| $m$        | 3.9   | $Kg$    | $b$            | $8.4e-4$ | $N.s^2$   | $Y_v$      | -6.06 | -        |
| $I_{xx}$   | 0.082 | $N.m^2$ | $d$            | $4.4e-5$ | $N.m.s^2$ | $N_f$      | -0.12 | -        |
| $I_{yy}$   | 0.082 | $N.m^2$ | $R$            | 0.12     | $m$       | $X_u$      | -5.7  | -        |
| $I_{zz}$   | 0.140 | $N.m^2$ | $L$            | 0.24     | $m$       | $Y_v$      | -4.3  | -        |
| $l$        | 0.2   | $m$     | $B_y$          | 0.12     | $m$       | $N_r$      | -0.32 | -        |
| $g$        | 9.8   | $m/s^2$ | $X_{\ddot{u}}$ | -2.45    | -         | $\rho_w$   | 1000  | $Kg/m^3$ |

to point in xy, xz, yz plane”, Fig. 22 “show position response of the robot in x, y, z axis”, Fig.23 “show attitude response around x, y, z axis”, Fig.24 “show the desired input of forces and moments” and Fig. 29 “show the flying trajectory response in 3D during different stages of time”), Mobile system (are shown in the following: Fig.20 “show the trajectory response of moving the mobile robot from point to point in xy plane”, Fig. 25 “show position and heading response of the robot in x, y and around z”, Fig. 27 “show input response of the right and left motors” and Fig.29 “show the mobile trajectory response in 3D during different stages of time”) and Sailing system (are shown in the following: Fig. 21 “show the trajectory response of moving the sailing robot from point to point in xy plane”, Fig. 26 “show position and heading response in x, y and around z”, Fig. 28 “show input response of the right and left pumps” and Fig. 29 “show the sailing trajectory response in 3D during different stages of time”).

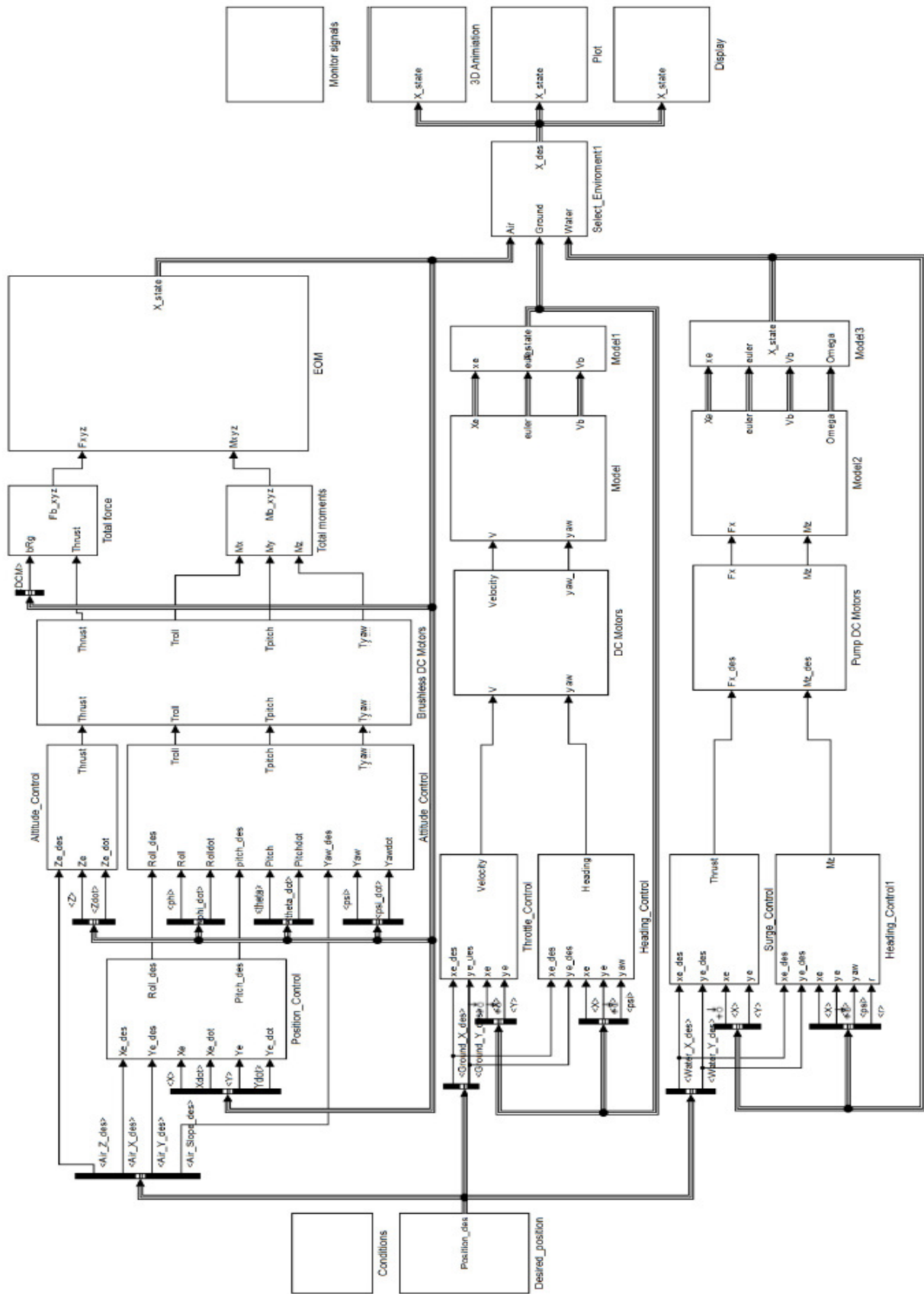


Fig. 18. SIMULINK BLOCKS

TABLE 3. CONTROL GAINS

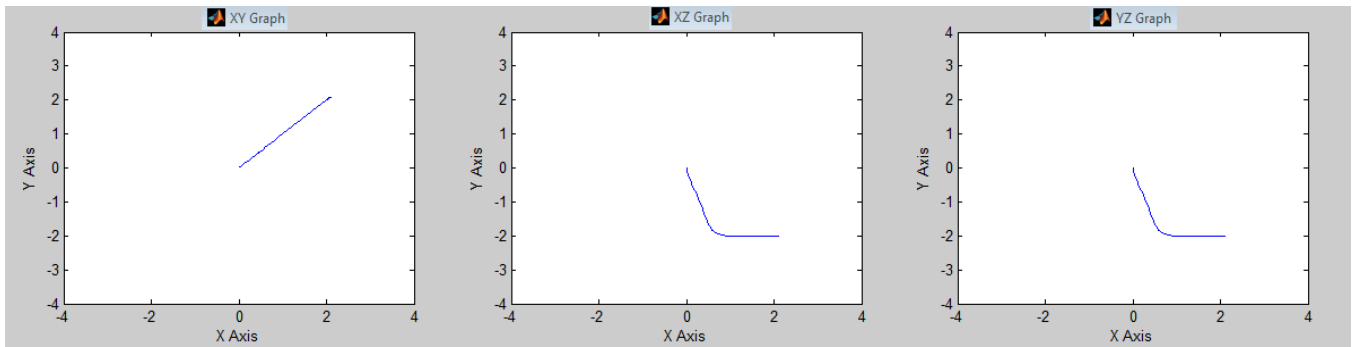
| Systems | Control Gains  |     |                |       |                |       |                   |      |                     |      |                   |   |
|---------|----------------|-----|----------------|-------|----------------|-------|-------------------|------|---------------------|------|-------------------|---|
| Flying  | $K_{pz}$       | 2.5 | $K_{pX}$       | 0.5   | $K_{pY}$       | 0.5   | $K_{p\phi}$       | 5.15 | $K_{p\theta}$       | 5.15 | $K_{p\psi}$       | 2 |
|         | $K_{p\dot{z}}$ | 300 | $K_{p\dot{X}}$ | 0.102 | $K_{p\dot{Y}}$ | 0.102 | $K_{p\dot{\phi}}$ | 1.6  | $K_{p\dot{\theta}}$ | 1.6  | $K_{p\dot{\psi}}$ | 1 |
| Mobile  | $K_{ptXY}$     | 2   | $K_{phXY}$     | 1     | -              | -     | -                 | -    | -                   | -    | -                 | - |
| Sailing | $K_{ptXY}$     | 2   | $K_{pa}$       | 1     | $K_{phXY}$     | 1     | $K_{p\psi}$       | 1    | $K_{p\dot{\psi}}$   | 0.2  | -                 | - |

TABLE 4. SYSTEM SATURATIONS

| Systems | System Saturations |             |                |                 |                |                     |                |           |
|---------|--------------------|-------------|----------------|-----------------|----------------|---------------------|----------------|-----------|
| Flying  | $F_{Tdes}$         | 0to-47.04N  | $M_{actx des}$ | -3to3N.m        | $M_{acty des}$ | -3to3N.m            | $M_{actz des}$ | -3to3N.m  |
|         | $X_{des}$          | -10 to 10 m | $Y_{des}$      | -10to10m        | $Z_{des}$      | 0 to -5 m           | -              | -         |
| Mobile  | $u_{des}$          | -2 to 2 m/s | $\psi_{des}$   | $-\pi, \pi$ rad | $\omega_r$     | 0to26 r/s           | $\omega_r$     | 0to26 r/s |
| Sailing | $F_{act des}$      | 0 to 2 N    | $M_{actz des}$ | -0.9to0.9N.m    | $u_{des}$      | 0to2 m/s            | -              | -         |
|         | $X_{des}$          | -10 to 10 m | $Y_{des}$      | -10to10m        | $\psi_{des}$   | $-\pi$ to $\pi$ rad | -              | -         |

TABLE 5. SIMULATION SYSTEM TEST RESULTS

|                   | Position/<br>Heading | initial<br>value | desired<br>value | final<br>value | rise<br>time | delay<br>time | steady<br>state time | overshoot |
|-------------------|----------------------|------------------|------------------|----------------|--------------|---------------|----------------------|-----------|
| Flying<br>system  | Z                    | 0                | -2               | -2             | 1.5          | 0.7           | 1                    | 1.9       |
|                   | X                    | 0                | 2                | 2              | 2.8          | 2             | 3.9                  | 4         |
|                   | Y                    | 0                | 2                | 2              | 2.8          | 2             | 3.9                  | 4         |
| Mobile<br>system  | X                    | 0                | 8                | 8.04           | 4.4          | 3.55          | 6.1                  | 0.5       |
|                   | Y                    | 0                | 8                | 8              | 4.9          | 3.25          | 6.1                  | 0         |
|                   | psi                  | Pi               | -                | -              | -            | -             | -                    | -         |
| Sailing<br>system | X                    | 0                | 5                | 5              | 17.6         | 11.55         | 23.8                 | 0         |
|                   | Y                    | 0                | 5                | 5              | 15.9         | 13.8          | 28.4                 | 0         |
|                   | psi                  | 0                | -                | -              | -            | -             | -                    | -         |



Flying system: Trajectory response under controller (Moving from point to point) in 2D “xy, xz, yz plane”.

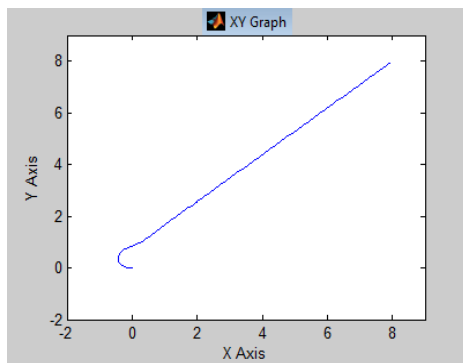


Fig. 19. Mobile system: Trajectory response under controller (Moving from point to point) in xy Plane.

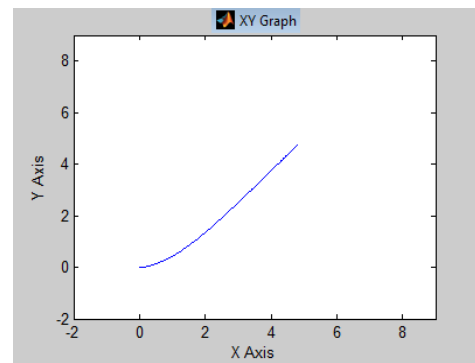


Fig. 20. Sailing system: Trajectory response under controller (Moving from point to point) in xy Plane.

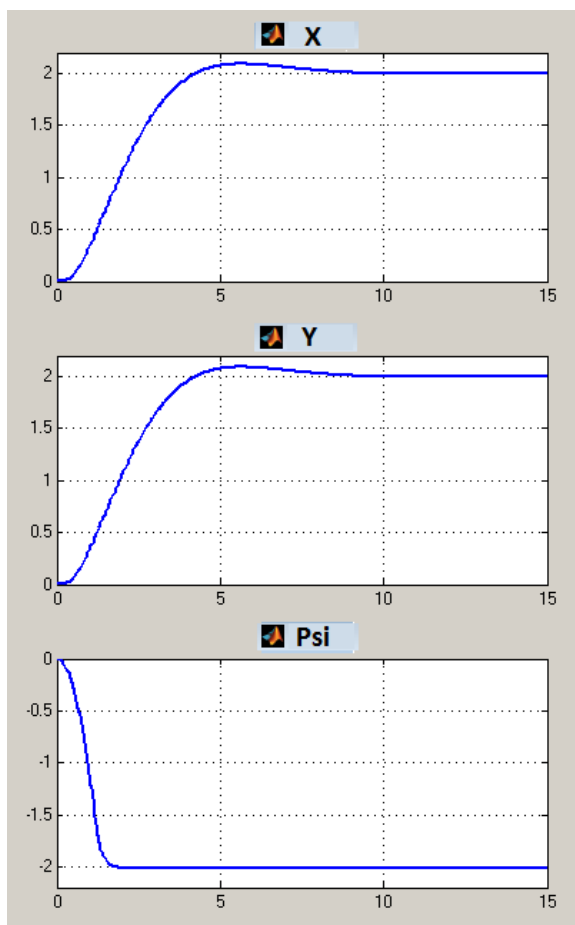


Fig. 21. Flying system: position response (X,Y,Z “meter” / time “sec”)

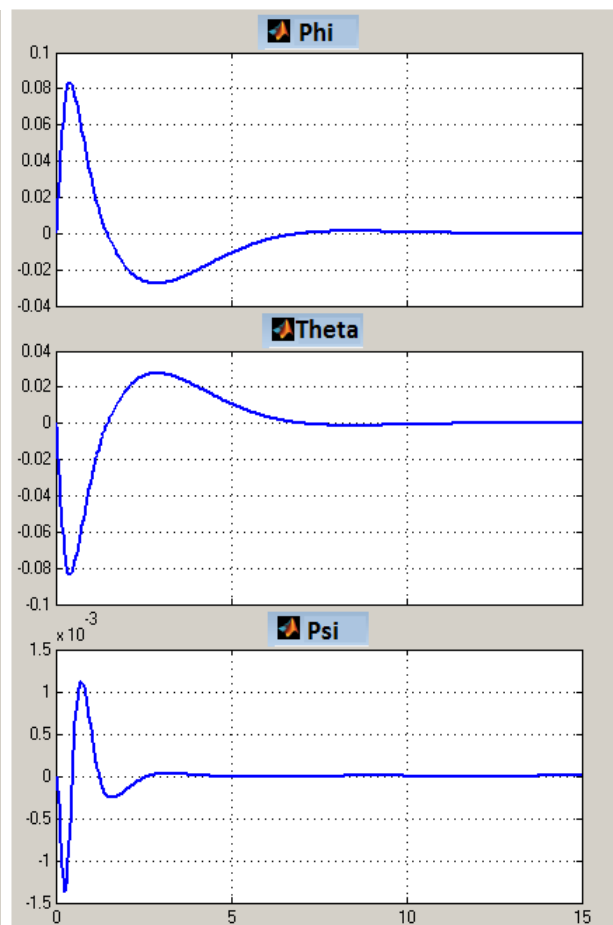


Fig. 22. Flying system: attitude response ( $\phi, \Theta, \psi$  “rad” /time “sec”)

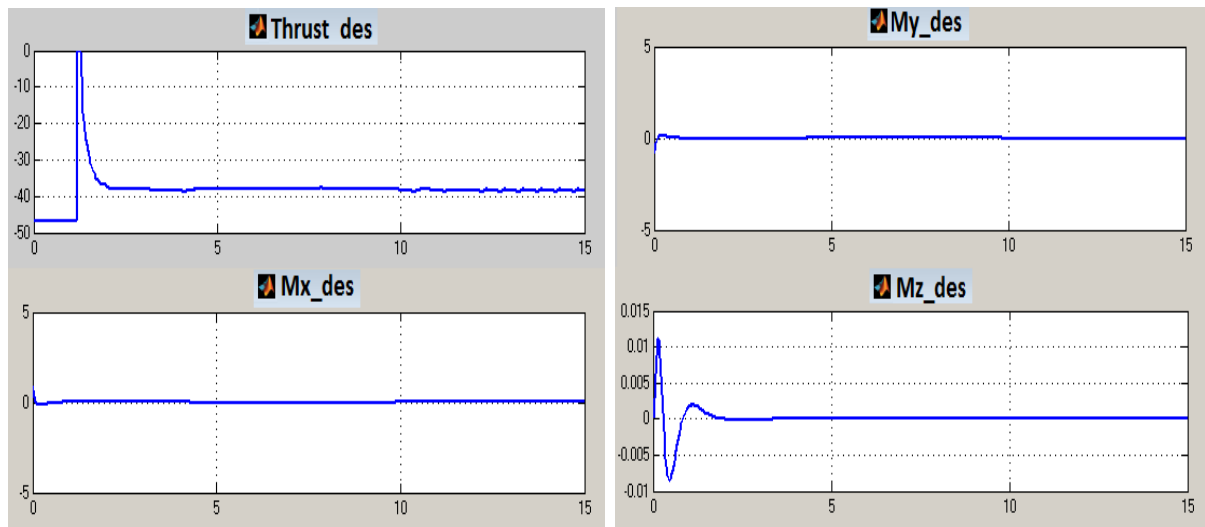


Fig. 23. Flying system: desired input ( $F_{Tdes}$  "N" / time "sec"), ( $M_{actx\_des}$ ,  $M_{acty\_des}$ ,  $M_{actz\_des}$  "N.m" / time "sec")

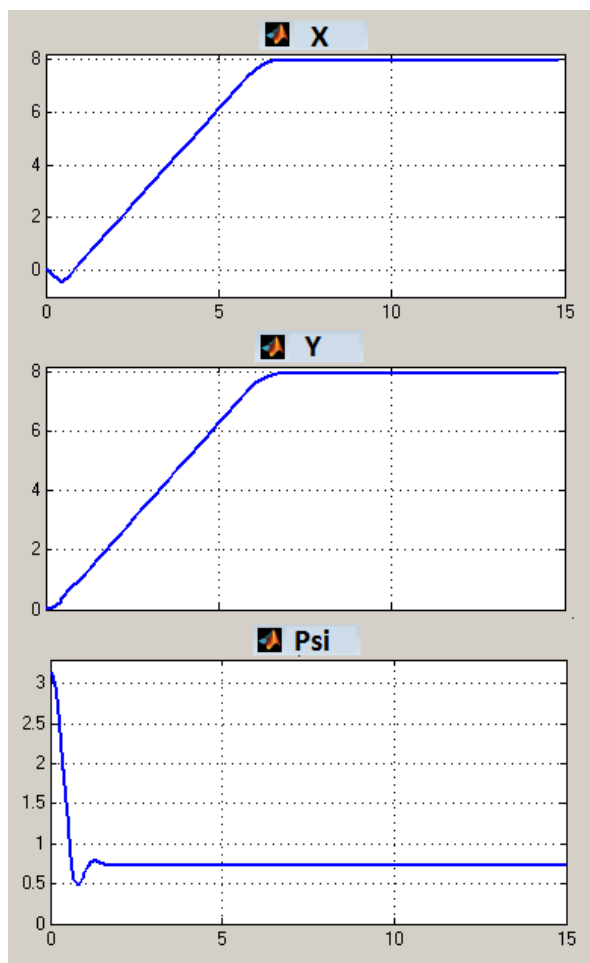


Fig. 24. Mobile system: position and heading response (X,Y "meter" / time "sec"), ( $\psi$  "rad" / time "sec")

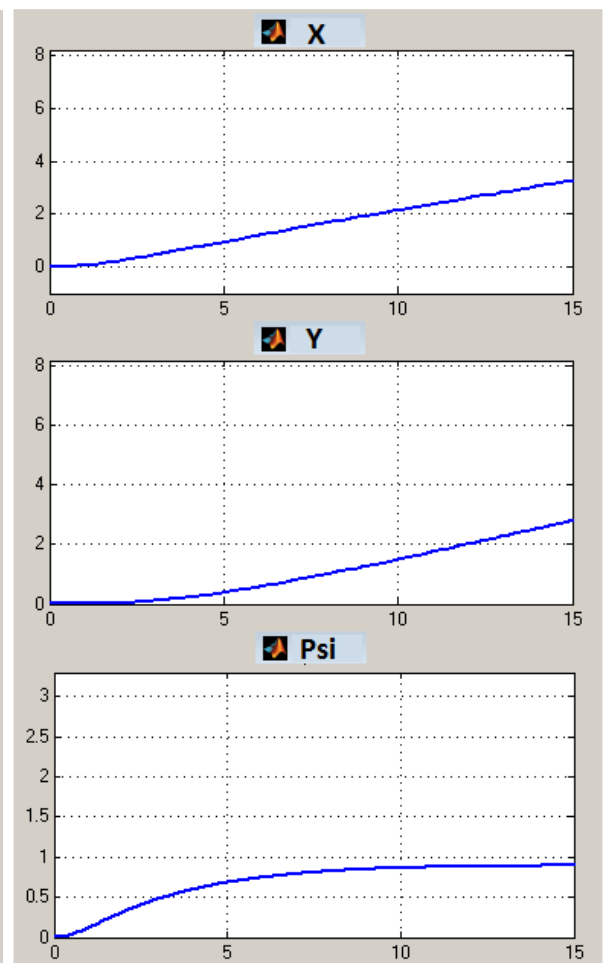


Fig. 25. Sailing system: position and heading response (X,Y "meter" / time "sec"), ( $\psi$  "rad" / time "sec")

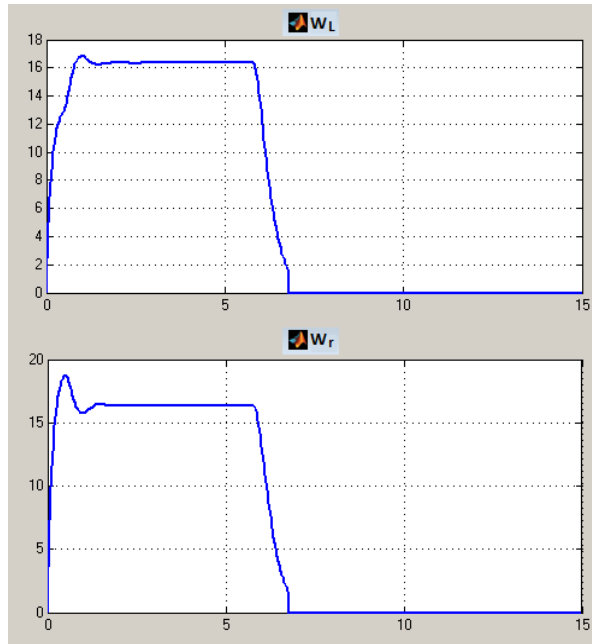
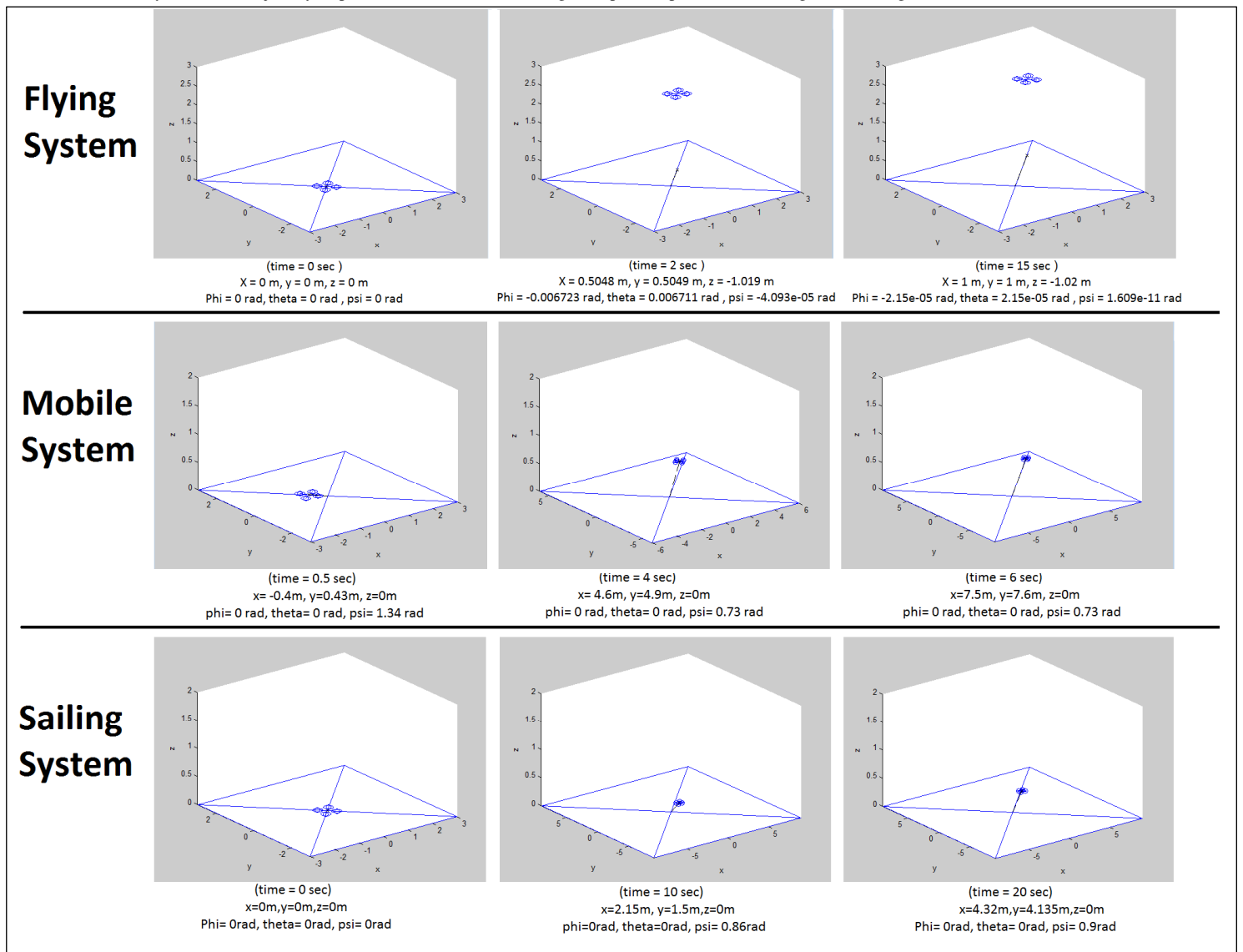


Fig. 26. Mobile system: input response ( $w_l, w_r$  "r/s"/ time "sec")



Fig. 27. Sailing system: input response ( $F_p, F_{stb}$  "N" / time "sec")

Total system test: Trajectory response under controller (Moving from point to point) in 3D during different stages of time.



## CONCLUSION

This research focuses on designing an autonomous different environment robot. Firstly, the mathematical models for the autonomous different environment robot dynamics and kinematics are derived. The environments are driven in one module because of using the same axis which seems to be easier to control. The dynamics model is derived using Newton-Euler law. Then a linearized version of the model is obtained. After that, a PID controller is designed using nested control loops and applied to the model. Finally the behavior of the Robot under the proposed control strategy is observed in 3D plot Simulink.

## REFERENCES

- [1] Luis Rodolfo García Carrillo, Quad Rotorcraft Control Vision-Based Hovering and Navigation, Springer, 2013, pp. 23-34
- [2] Peter Corke, Robotics, vision and control fundamental algorithms in MATLAB, Springer, 2011, pp. 65-78, 78-84
- [3] Thor Fossen, Handbook Of Marine Craft Hydrodynamics And Motion Control, John Wiley & Sons, 2011, pp. 3-14,15-19, 109-132
- [4] Do Thanh Sen, Determination of Added Mass and Inertia Moment of Marine Ships Moving in 6 Degrees of Freedom, International Journal of Transportation Engineering and Technology, 2016, pp. 8-13
- [5] Katsuhiko Ogata, Modern Control Engineering Fifth Edition, Pearson , 2010, pp. 567-570
- [6] Samir Bouabdallah, design and control of quadrotors with application to autonomous flying, Lausanne EPFL, 2007, pp. 15-24, 77, 95-106
- [7] Peter H. Zipfel, Modeling and Simulation of Aerospace Vehicle Dynamics Second Edition, AIAA EDUCATION SERIES, 2007, pp. 75-76
- [8] Vicente Martínez, Modelling of the Flight Dynamics of a Quadrotor Helicopter, CRANFIELD UNIVERSITY, 2007, pp. 38-56
- [9] Teppo Luukkonen, Modeling and control of quadcopter, Independent research project in applied mathematics, Aalto University school of Science, 2011, pp. 2-7,10-20
- [10] Francesco Sabatino, Quadrotor control: modeling, nonlinear control design, and simulation, Master's Degree Project Stockholm sweden 2015, pp. 7-24
- [11] Thor I. Fossen, Guidance and Control of Ocean Vehicles, Wiley, 1994, pp. 5-7, 25-47
- [12] Thor I. Fossen, Marine Control Systems Guidance, Navigation, and Control of Ships, Rigs and Underwater Vehicles-Marine Cybernetics, Trondheim, Norway, marine cybernetics, 2002, pp 9-12, 17-29, 57-64
- [13] Alexander I. Korotkin, Add mass of ship structure, springer, 2007, pp. 131-137, 360-379
- [14] H. L. Chan, International Journal of Mechanical Engineering and Robotics research Vol. 4 No. 4, October 2015, pp. 287--291
- [15] Heba\_ElKholy, Dynamic Modeling and Control of a Quadrotor Using Linear and Nonlinear Approaches, AUC, 2014, pp. 27-43
- [16] Jyotsna Pandey, Study on Manoeuverability and Control of an Autonomous Wave Adaptive Modular Vessel (WAMV) for Ocean Observation, International Association of Institutes of Navigation World Congress Prague, Czech Republic, 20–23 October 2015.

- [17] Edoardo I.Sarda, Station-keeping control of an unmanned surface vehicle exposed to current and wind disturbances, 2016, pp. 1-44
- [18] Wilhelm B. Klinger, Control of an Unmanned Surface Vehicle with Uncertain Displacement and Drag, IEEE (OES), 2016, pp. 1-17
- [19] Sin-Der Lee, Design and experiment of a small boat auto-berthing control system, 12th International Conference on ITS Telecommunications, 2012, pp. 397-401
- [20] H. Yasukawa, Introduction of MMG standard method for ship maneuvering Predictions, J Mar Sci Technol springer, 2015, pp. 37-52
- [21] Hashem Ashrafiuon, Sliding Mode Tracking Control of Surface Vessels, American Control Conference USA, June 11-13 2008, pp.556-561
- [22] Christian R. Sonnenburg, Modeling, Identification, and Control of an Unmanned Surface Vehicle, Doctor of Philosophy In Aerospace Engineering Faculty of the Virginia Polytechnic Institute and State University, paper number or journal number, 2012, pp. 38-60,101
- [23] Petr Švec, Dynamics-Aware Target Following for an Autonomous Surface Vehicle Operating under COLREGs in Civilian Traffic, IEEE/RSJ International Conference on Intelligent Robots and Systems IROS, November 3-7, 2013, pp. 3871-3878
- [24] Stephen Armah, Implementation Of Autonomous Navigation Algorithms On Two-Wheeled Ground Mobile Robot, American Journal of Engineering and Applied Sciences, 2014, pp. 149-164